An empirical equation for inlet flushing capacity

A. E. El-Ansary [a], K. H. Baghdady [a], M. A. El-Mooty [a] and Y. M. M. Gewilli [b]
[a]*Hydraulic and Irrigation Dept., Faculty of Eng., Alexandria University, Alexandra, Egypt*
[b]*Coastal Research Institute – National Water Research Center, Alexandria, Egypt*

Factors controlling the stability of tidal inlet cross-sections were discussed. These factors were analyzed dimensionally considering hydraulic and geometrical parameters. From this analysis, dimensionless function was developed concerning tidal inlet flushing capacity. In order to transform this function to applicable equation, a numerical model was developed and checked with field data. This model is used to calculate inlet channel velocity, bay water level, tidal prism, sediment transport through inlet channel, flushing capacity and Keulegan's coefficient. The sediment transport is calculated using equations of Engelund-Hansen and Van-Rijn. The numerical model is also used to explain the behavior of the dimensionless parameters in the developed function. By means of multi regression method and using the results of 2550 model runs of stable tidal inlet, a relationship for tidal inlet flushing capacity in terms of maximum mean inlet discharge, inlet Froude number, relative channel length and relative grain size was obtained. The results of the flushing capacity equation were compared to field data and a good agreement was found. The developed equation is presented in two families of curves, so that the flushing capacity can be determined easily.

في هذا البحث، تم عرض ودرا سة العوامل المؤثرة فى اتزان مداخل المد. هذه العوامل تم تحليلها بعديـــا آخذيـــن فـــى الأعتبـــار العوامل الهيدروليكية والعوامل الخاصة بخصائص الرسوبيات. من هذا التحليل تم اسنتاج دالة لحساب الســـعة التطهيريـــة لمداخـــل المد. لكى نحول هذه الدالة الى معادلة قابلة للتطبيق، تم انشاء نموذج عددى وتم اختبارة بالبيانات الحقليـــة. هـــذا البرنـــامج يقـــوم بحساب السرعات ،التصرفات خلال مداخل المد، المنشور المدى، حركة الرسوبيات والسعة التطهيرية لمداخل المد. كذلك يســـتخدم هذا البرنامج لدراسة تأثير كل عامل من العوامل فى الدالة المستنتجة. بعد ذلك تم تجرية هذا البرنامج ٢٥٥٠ مرة لدراسة حـــالات مداخل مد متزنة. من نتائج هذه الحالات تم اسنتاج معادلة لحساب السعة التطهيرية لمداخل المد. بمقارنة هذه المعادلـــة بالقياســـات الحقلية وجد أنها تعطى نتائج جيدة.

Keywords: Tide, Tidal inlet, Sediment transport, Numerical models, Flushing capacity

1. Introduction

The tidal inlet connects lagoon/bay to coastal oceans or seas. It provides many benefits, like navigational access to the lagoon/bay for commercial shipping, fishing, and recreational boating. Also the tidal prism flows through inlet during tidal cycle playing a dominant role in flushing the sediments from the inlet and maintaining the water quality and salinity level in the lagoon/bay.

The main parameters affecting the stability of tidal inlets are: tide and fresh water discharge in the lagoon as a flushing parameter and the littoral drift as a filling parameter. The inlet morphology and surface area of the lagoon are also affecting the inlet stability. To keep the inlet stable against closure without maintenance dredging, it is essential that the inlet should satisfy the requirements of the inlet stability curve of Escoffier [1], fig. 1. In this curve, the maximum velocity through an inlet increases with cross-sectional area. It reaches the peak value at the critical cross-sectional area, A_c^* and then decreases for larger cross-sectional areas. This means that the inlet should fall on the stable side of the peak. The associated velocity should also be in accordance with Bruun's relationship [2], which is 0.8m/sec. $< V_{max.-mean} <$ 1.2 m/sec. The better inlet condition is the ability of the tidal flow to flush out the sediment that are carried by the waves and currents action to the inlet. These principles are very important and should be taken into consideration during the design of tidal inlets.

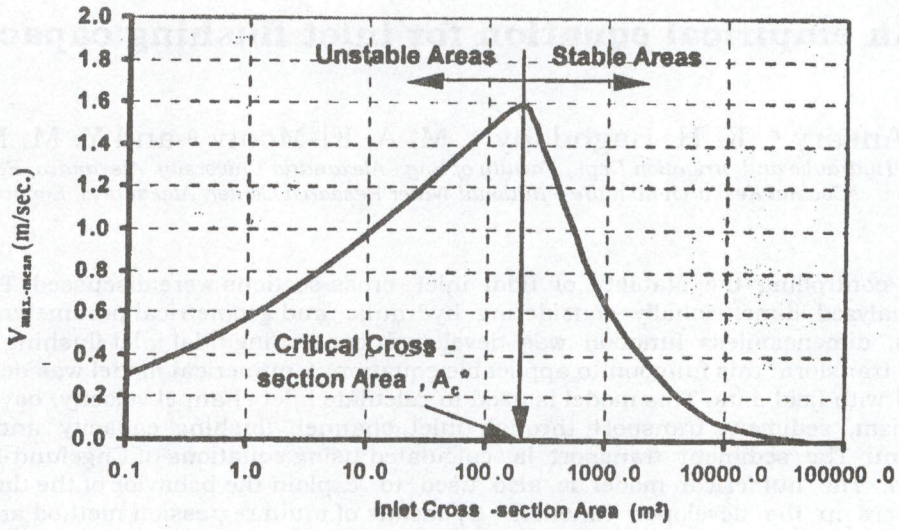

Fig. 1. Illustration of escoffier's stability concept.

In the field, it is easy to measure all the hydraulic conditions of the tidal inlet such as (i.e. velocity, tidal prism), but it is difficult to measure the flushing capacity of tidal inlet. Therefore, it is very important to develop an equation to determine the flushing capacity of tidal inlet.

The main objective of this paper is to develop an empirical equation to determine the flushing capacity through tidal inlet.

2. Background

From measured values, Bruun [2] proposed a theory of the tidal inlet stability as a function of tidal prism P_s contra the sediment inflow M_{tot} from the sea. The flow in the channel must not only be able to handle local sediment transport but must also be able to flush extra sediment out of the channel. The extra sediment is carried to the channel by waves, currents and by erosion of the banks. P_s is defined as the spring tidal prism in m^3 each half tidal period and M_{tot} is the total drift of sediment towards the entrance in m^3/year. Bruun summarized the inlet conditions in relation to P_s/M_{tot} , for semi-diurnal tide, to be as shown in table 1.

Van de Kreeke's [3], characterized the stability of tidal inlets by the maximum of the bed shear stress during tidal cycle. He found that, from field measurements, the bed shear stress for stable tidal inlet is between (0.36 and 0.56) kg/cm².

3. Factors affecting the stability of tidal inlets

The stability of tidal inlets depends mainly on the following factors, see fig. 2.

(a) The tidal range ($2a_o$): The tidal range is the height between successive high and low sea levels. The tide range affects the gradient of water surface and also the flow in and out of the inlet channel. The tide range is represented by the spring tidal range ($2a_{os}$)

(b) The types of tide: It can be either semi-diurnal, diurnal or mixed tides. The type of tide indicates the shape and tidal period (T_p).

(c) The inlet cross-section area (A_c): A large cross-sectional area means a large discharge capacity.

(d) The length of inlet channel (L_c): A long channel will cause an increased resistance against the tidal flow.

(e) The lagoon/bay surface area (A_{bay}): A large lagoon/bay surface area will respond less to tide than a small one.

(f) Fresh water discharge to the lagoon/bay (Q_f): Fresh water discharge into the lagoon/bay decreases the flood flow and increases the ebb flow.

Table 1
Inlet conditions in relation to P_s/M_{tot}

P_s/M_{tot}	Entrance conditions
$300<P_s/M_{tot}$	Little or no ocean bar out side inlet channel (ocean shoal may occur further out)
$150<P_s/M_{tot}<300$	Condition are good, very good flushing and minor bar formation.
$100<P_s/M_{tot}<150$	Low ocean bar, navigation problems usually minor.
$50<P_s/M_{tot}<100$	Rather larger bar by the entrance but usually a channel through the bar
$20<P_s/M_{tot}<50$	Typical bar by-passers get flushed by the increased water discharge during storms and monsoons.
$P_s/M_{tot}<20$	Very unstable inlets, mainly just overflow channels.

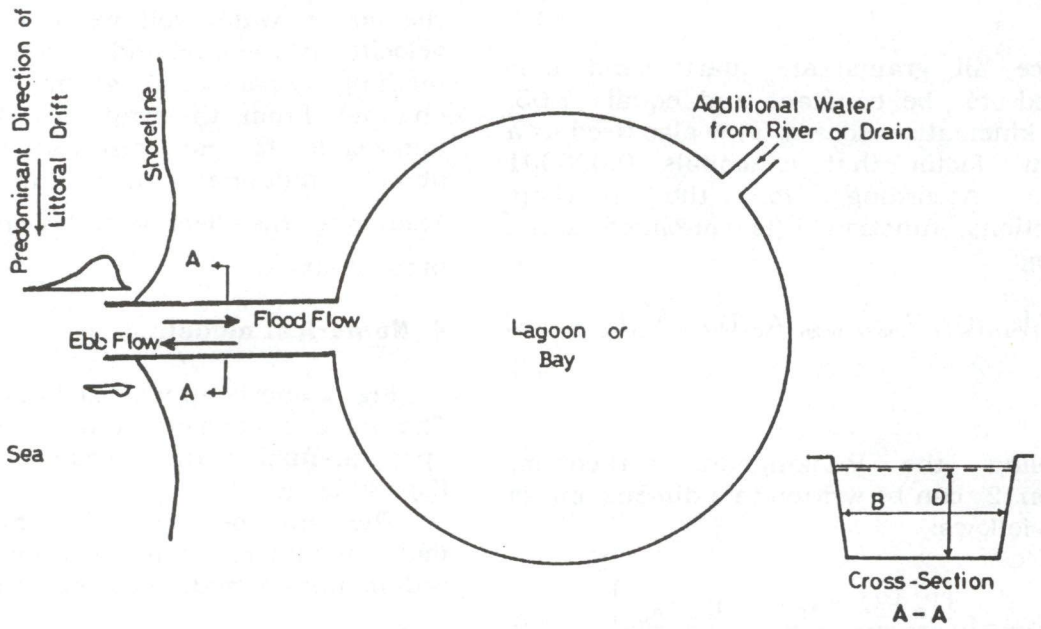

Fig.2. Idealized inlet-bay system.

(g) Filling factor (M_{tot})*:* The littoral drift may fill the inlet entrance. The rate of littoral drift is affected by waves, longshore currents, grain size and the orientation of bottom contour and shoreline to the incoming waves. The total littoral drift, M_{tot} , towards the inlet during one year is the filling parameter used in this study. The aim of using this parameter is to compare the flushing capacity of the inlet.

(h) Other minor factors: Other factors such as wind stress in the bay and inlet surface radiation stress and coriolis effects are neglected in the present study.

The flushing capacity of the tidal inlets may be characterized by the following.

3.1. Hydraulic conditions

Those include the following factors, see fig. 2:

i. The spring tidal range ($2a_{os}$).
ii. The fresh water discharge to the lagoon/bay (Q_f).
iii. The maximum-mean velocity ($V_{max\text{-}mean}$).
iv. The cross-section area of tidal inlet (A_c).
v. The depth of inlet channel (D).
vi. The Length of Channel (L_c).
vii. The spring tidal prism (P_s).
viii. The tidal period (T_p).
ix. Gravitational acceleration (g).
x. Water kinematic viscosity (υ).

3.2. Sediment properties

Those include the following factors:

i. The mean particle size (d_{50}).
ii. The relative density of sediment (s).

3.3. Dimensional analysis

Relating to the previous factors, the flushing capacity, M_{flu}, can be expressed as follows:

$$M_{flu} = f_1(a_{os}, Q_f, V_{max-mean}, A_c, D, P_s, T_p, L_c, g, d_{50}, \upsilon, s) \quad (1)$$

Since all grains are quartz sand, s is assumed to be constant and equals 2.65. Water kinematic viscosity (υ) is also used as a constant factor that is equals 0.000001 m^2/sec. According to the previous assumptions, function 1 is simplified to the following:

$$M_{flu} = f_1(a_{os}, Q_f, V_{max-mean}, A_c, D, P_s, T_p, L_c, g, d_{50}) \quad (2)$$

Appling the Buckingham π-theorem, Function 2 can be written in a dimensionless form as follows:

$$\frac{M_{flu}}{Q_{max-mean}} = f_1\left\{\frac{P_s + Q_f \times T_p}{A_c \sqrt{g.D}\, T_p}, \frac{D}{d_{50}}, \frac{a_{os}}{L_c}\right\}, \quad (3)$$

where;

$\frac{P_s + Q_f \times T_p}{Q_{max-mean}}$ is the ebb tidal prism, $= V_{max-mean} . A_c$,

$\frac{M_{flu}}{Q_{max-mean}}$ is the relative flushing capacity,

$\frac{P_s + Q_f \times T_p}{A_c \sqrt{g.D}\, T_p}$ is the inlet Froude number (case of tide and freshwater discharge),

$\frac{P_s}{A_c \sqrt{g.D}\, T_p}$ is the inlet Froude number (case of tide only),

$\frac{D}{d_{50}}$ is the relative grain size, and

$\frac{a_{os}}{L_c}$ is the relative channel length.

Function 3 expresses the dimensionless inlet flushing capacity of tidal inlet in terms of maximum-mean inlet discharge, inlet Froude number, relative channel length, and relative grain size. This function takes the effect of tide plus freshwater discharge to the lagoon /bay. The flushing ability will be enhanced due to the additional discharge (Q_f). This is due to the extra water volume that increases the velocity in the inlet and thereby increases the flushing capacity of sediment in the inlet channel. From the available data, it has been impossible to gain any assure information about additional inflow to the system. Therefore, the effect of (Q_f) is not taken in the present study.

4. Numerical modeling

Fig. 2 shows an idealized inlet-bay system. The inlet is considered to be similar to an open channel with a cross-section (A_c), depth (D) and length (L_c).

The developed numerical model has two main modules; hydrodynamic module and sedimentation module as shown in fig. 3.

4.1. The hydrodynamic module

This model is based on one-dimensional momentum equation for the inlet and a continuity equation for the bay.

4.1.1. The momentum equation

The momentum equation in one dimensional form for the inlet channel can be expressed as the following:

$$\frac{\partial u}{\partial t} + u\frac{\partial u}{\partial x} = -g\frac{\partial a_s}{\partial x} - g\frac{u|u|n^2}{R_c^{4/3}}, \quad (4)$$

where; u is the average flow velocity in the inlet channel, a_s is the elevation of water level due to tide, n is Manning coefficient, R_c is the

hydraulic radius and g is the acceleration of gravity.

4.1.2. The continuity equation

The rate of change of water level in the lagoon/bay is a function of inlet discharge plus discharges into the bay from other sources. This phenomenon can be described by a simple mass continuity equation as follows:

$$\frac{\partial a_b}{\partial t} = \frac{Q_t}{A_{bay}} + \frac{Q_f}{A_{bay}} . \qquad (5)$$

Where; A_{bay} is the surface area of the bay, Q_i is the discharge of i^{th} inlet, Q_f is the discharge into the bay from other sources such as (rivers, pumped inflows, etc.), Q_t is the total inlets discharge and is calculated using the following equation:

$$Q_t = \sum_{i=1}^{n} Q_i \qquad (6)$$

4.2. The sedimentation module

In this model, two equations of Engelund-Hansen [4] and Van-rijn [5, 6, 7] are used to compute the rate of sediment transport in the channel based on the average flow velocity from the hydrodynamic model at each time step. The average of these equations is obtained to get the volume of sediment transport in the channel.

4.2.1. Flushing capacity subroutine

Flushing capacity, (M_{flu}), of the inlet channel is defined as the total sediment flushed by the ebb flow through inlet during one year. According to this definition, the flushing capacity can be determined by the following equation:

$$M_{flu} = 365 \times \frac{24}{T_p} \times \left(\sum_{i=1}^{nt} q_{s_i} \times B \right) \Big/ 14.0 . \qquad (7)$$

Where; q_{s_i} is the sediment flushed by the ebb flow ($m^3/m/T_e$), T_e is the ebb time as a part of the tidal period, T_p is the tidal period, (B) is the inlet channel width, a_{os} is the spring tide amplitude, a_{on} is the neap tide amplitude and is taken as (0.4 a_{os}), when data is not available, (Bruun [8]), and nt is the number of ebb cycles between successive two spring tides which takes place each 14 days.

The tide amplitude between spring (a_{os}) and neap (a_{on}) is calculated using the following equation:

$$a_s = \frac{(a_{os} + a_{on})}{2.0} + \frac{(a_{os} - a_{on})}{2.0} \cos\left(\frac{2 \times \pi \times t}{T_l / 2.0} \right) . \qquad (8)$$

Where; T_l is the lunar period and equals 28 days.

Fig. 4 gives typical tide at El-Arish and Damietta harbor for the period from 21 August to 18 Sep. 1997.

The input data required for running the model are: tidal range, tidal period, length of channel, surface area of lagoon/bay, fresh water discharge, cross-sectional area of the inlet channel and grain size of the inlet bed. The flow chart of this numerical modeling is given in fig. 3.

4.3. The boundary conditions

The boundary conditions of this system are the tidal water level variation in the sea, and the water level variation in the lagoon/bay. The program initiates when the water level in the sea and the bay equals zero. If the water surface in the lagoon/bay is assumed to remain horizontal all the times, the water discharge from the tidal flow through the inlet together with extra separate inflow will cause a change in water level in the lagoon/bay. After about 10 tidal periods, the movement of the lagoon/bay water surface has a constant shape. So, the maximum mean velocity remain constant

4.4. Model calibration

The numerical model was run using the data in table 2. The relationship between the measured and the predicted velocity gives very good agreement as shown in fig. 5. The standard error of estimate for the used data is 5.3 cm/sec.

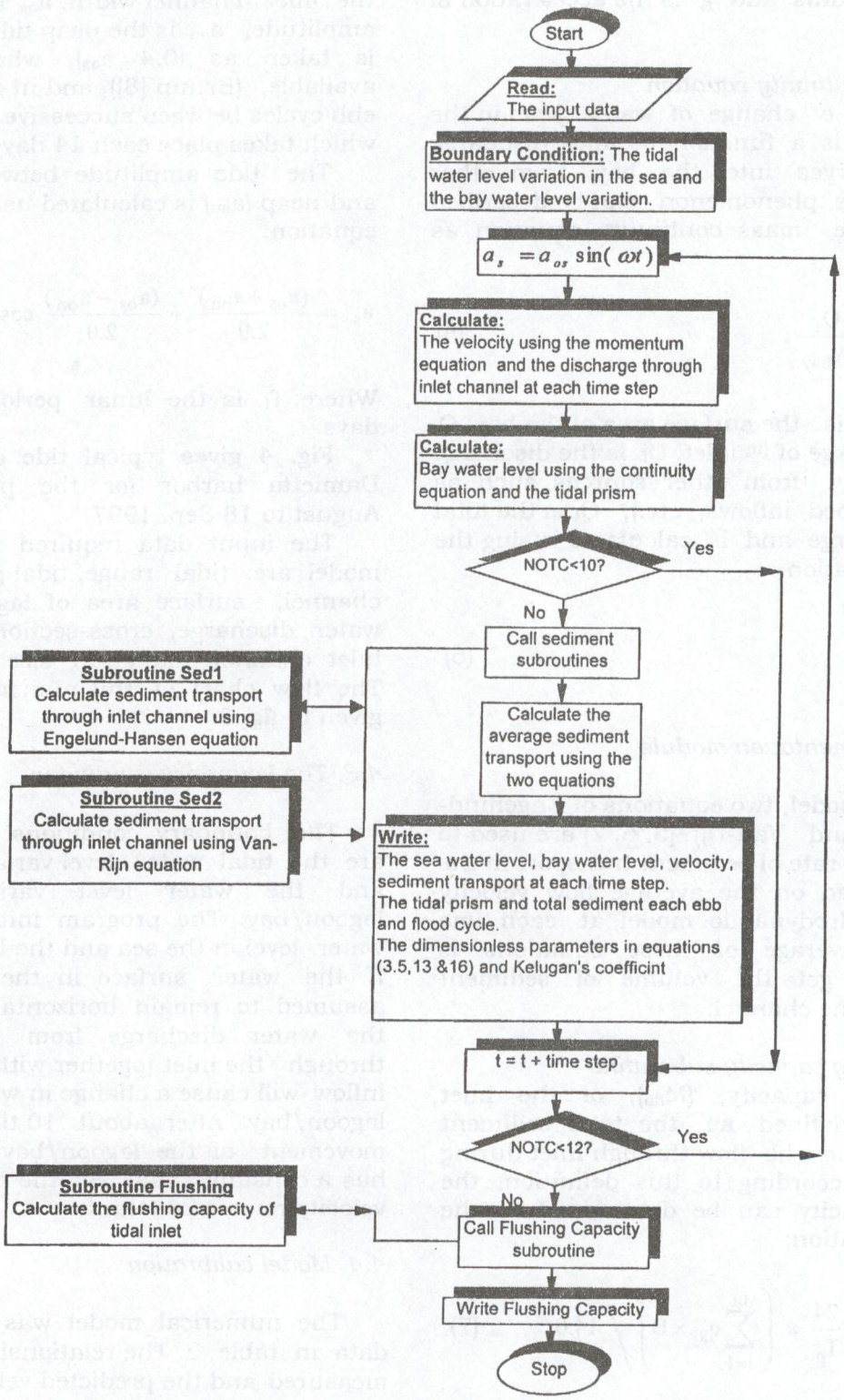

Fig. 3. Flow chart of tidal inlet numerical modeling.

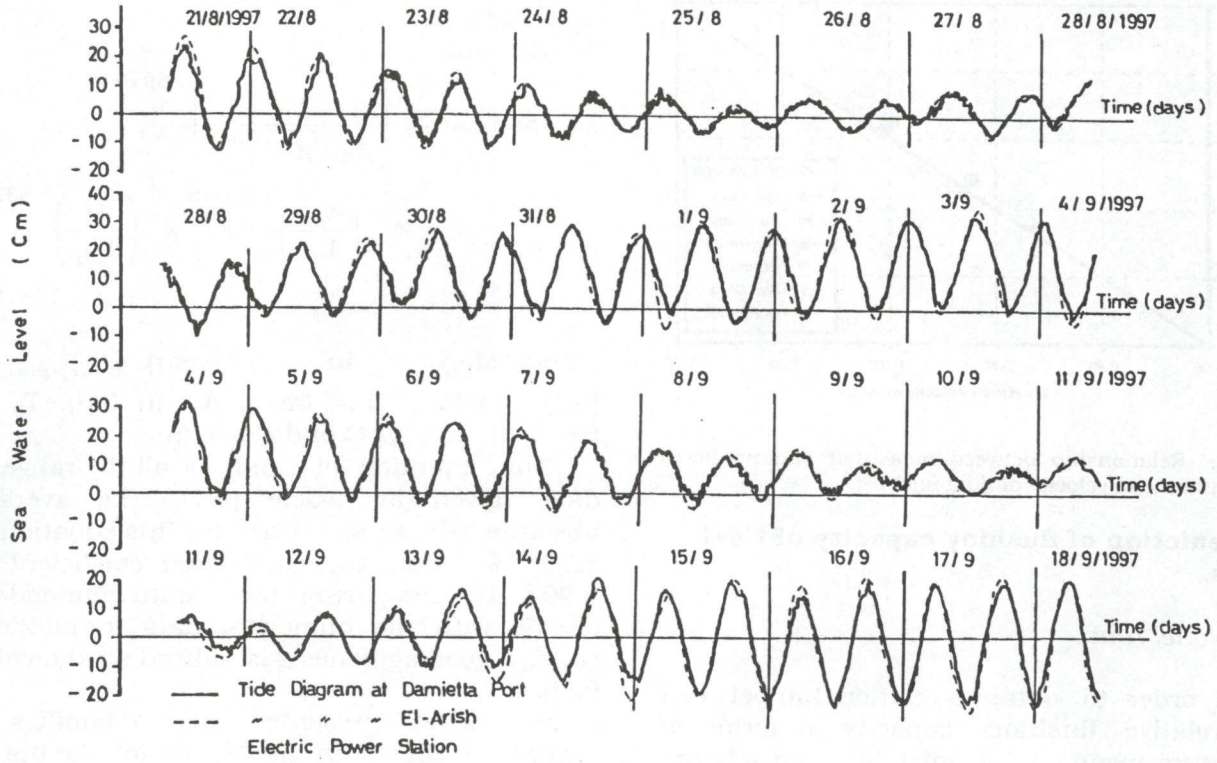

Fig. 4. Typical tide at El-Arish and Damietta harbor for the period from 21 August to 18 September 1997.

Table 2
Summary of the collected data of tidal inlets

Inlet	A_c (m^2)	D_{mean} (m)	W_{mean} (m)	A_{bay} (km^2)	L_c (m)	T_p (hours)	a_{os} (m)	M=1/n ($m^{1/3}$/sec.)	$V_{max.-mean}$	Country	Ref.
El-Bardawil	2414.0	6.3	383.0	585.0	700.0	12.40	0.20	_	0.89	Egypt	a
Rockaway	7650.0	8.2	933.0	57.5	8130.0	12.42	0.87	53.0	0.92	U.S.A.	b
Fire Iland	3298.0	4.3	792.0	228.0	10089.0	12.60	1.24	44.0	1.23	U.S.A.	b
Humboldt	6978.4	10.4	671.0	52.7	820.0	11.12	0.79	18.2	1.00	U.S.A.	b
San Digo	5915.0	12.5	565.0	44.1	5749.0	10.23	0.63	26.5	0.66	U.S.A.	b
St. Mary's	10353.0	10.0	1036.0	83.0	4633.0	8.86	1.02	25.4	1.19	U.S.A.	b
Thyboron	4864.0	8.0	608.0	180.0	3000.0	12.60	0.31	35.4	1.08	Denmark	c

(a) Data from CoRI [9]. (b) Data from O'Brien et al. [10].
(c) Data from Skou [11].

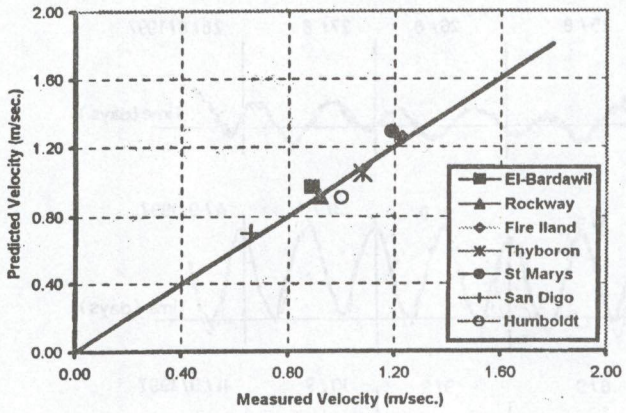

Fig. 5. Relationship between measured and predicted maximum mean velocity of tidal inlets.

5. Prediction of flushing capacity of tidal inlets

5.1. Model runs

In order to obtain a relationship between the relative flushing capacity in terms of maximum-mean inlet discharge ($M_{FLU}/Q_{max.-mean}$), inlet Froude number, Relative channel length and relative grain size as given in function 3, A 2550 numerical model runs were performed for the following cases.

- Tidal amplitude in the sea: a_{os} = (0.2, 0.3, 0.4, 0.5, 0.6 m)
- Depths: D = from 4.0 m to 9.0 m, each 0.25 m increment
- Tidal period: Semi-diurnal tide (T_p = 12.4 hour).

diurnal tide (T_p = 24.8 hour).

- Length of channel: L_c = (500, 1000, 1500 m).
- Grain sizes: d_{50} = (0.1, 0.2, 0.3, 0.4, 0.5 mm)

5.2. Empirical equation for the relative flushing capacity

Appling multi regression method, a relationship between relative flushing capacity in terms of maximum-mean inlet discharge ($M_{FLU}/Q_{max.-mean}$) and other parameters in the function 3 is presented in the following equation:

$$\frac{M_{FLU}}{Q_{max.-mean}} = 45850.44 \times \left(\frac{P_s}{A_c\sqrt{g \times D}\,T_p}\right)^{3.6916} \times \left(\frac{a_{os}}{L_c}\right)^{0.09615} \times \left(\frac{D}{d_{50}}\right)^{0.5375}, \quad (9)$$

where, M_{FLU} in (m^3/year), $Q_{max.-mean}$ in (m^3/sec.), P_s in (m^3), A_c in (m^2). T_p in (second), a_{os}, L_c, D and d_{50} in (m).

This equation is valid for all the range of data given in article (5.1). The average absolute percentage error for this equation is 8.73 % while the correlation coefficient is 0.993. By comparing the results obtained by eq. (9) with the numerical data for all 2550 runs, a good agreement is noticed as shown in fig 6.

Eq. 9 is presented by two families of curves as shown in fig. 7. From the upper curves, the value of the parameter $[(a_{os}/L_c)^{0.09615} \times (D/d_{50})^{0.5375}]$ is calculated using the relative channel length (a_{os}/L_c) and the relative grain size (D/d_{50}). From the lower curves, the relative flushing capacity is calculated using the value of the inlet Froude number and the value of the parameter $[(a_{os}/L_c)^{0.09615} \times (D/d_{50})^{0.5375}]$ which is calculated from the upper curves.

5.3. Comparison between estimated flushing capacity and field data

In table 1, Bruun [2], stated that the tidal inlets are in very good condition for (P_s/M_{tot}) greater than 150. For (P_s/M_{tot}) between 100 and 150, the inlet remains fairly stable. For (P_s/M_{tot}) less than 100, navigation problems will be increased. The parameter (P_s/M_{tot}) dose not exhibit the effect of different parameters controlling the stability. Therefore, it is not accurate to use as a predictive tool. Also, the bed shear stress, for stable tidal inlets, is between (0.36 and 0.56) kg/cm², Van de Kreeke's [3].

The ratio (P_s/M_{FLU}) was calculated for all the 2550 runs and it was found that all ratios are greater than 100. The average ratios of

(P_s/M_{FLU}) for all runs, which fulfill the condition of the bed shear stress were calculated and given in table 3 for different grain sizes. From the comparison, it is noticed that, there is a good agreement between the measured and the estimated ratios.

5.4. Effect of tidal amplitude, tidal period and length of channel on cross-section area and flushing capacity

Stable inlet cross-section area, relative flushing capacity and the corresponding flushing capacity were plotted versus inlet Froude number for different tidal amplitude, tidal period and inlet channel lengths as shown in fig. 8, 9 and 10 respectively. The aim of these relationships is to examine the effect of tidal amplitude, tidal period and length of inlet channel on the stable inlet cross-section area and the corresponding flushing capacity. The numerical model results were used and the flushing capacity is calculated using eq. (9). From fig. 8, it is noticed that the inlet cross-section area, relative flushing capacity and flushing capacity increase with the increase of tidal amplitude. This is because of increasing differences between water levels in the sea and the bay, which affect the inlet velocity. The inlet cross-section area and the flushing capacity decrease with the increase of tidal period as shown in fig. 9. This is due to decreasing inlet velocity. Also, from fig. 10, the inlet cross-section area, the relative flushing capacity and the flushing capacity decrease with the increase of length of channel. The cause of this incidence is that the friction losses increase with the increase of channel length.

5.5. Effect of changing cross-section area of tidal inlet by the width

The effect of changing cross-section area of tidal inlet by width on flushing capacity is shown in fig. 11 for tidal amplitude 0.2 m. In this figure, the calculated flushing capacities from eq. (9) for 1 km² bay surface area were plotted versus the inlet cross-section area for different depths. From fig. 11, it is noticed that, for the same cross-section area, the greater depth gives higher flushing capacities. Therefore, it is better to choose a large depth when designing stable tidal inlets. Also, the large depth gives sufficient trapping depth to account for sedimentation during storms until the inlet can flush it out and it is useful for navigation requirements.

Table 3
Calculated P_s/M_{FLU} for different grain sizes

d_{50} (mm)	0.06	0.1	0.2	0.3	0.4	0.5
P_s/M_{FLU}	101	133	192	239	283	318

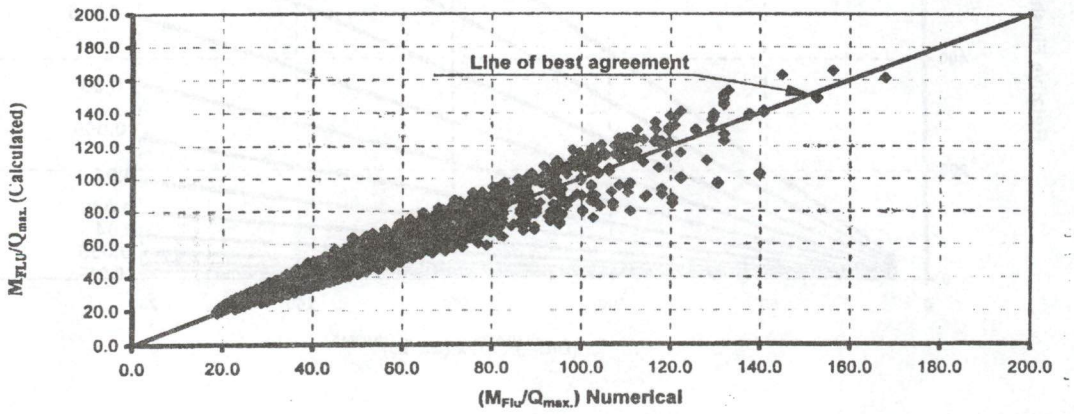

Fig. 6. Plot of calculated relative flushing capacity of stable tidal inlets versus the numerical values for all runs.

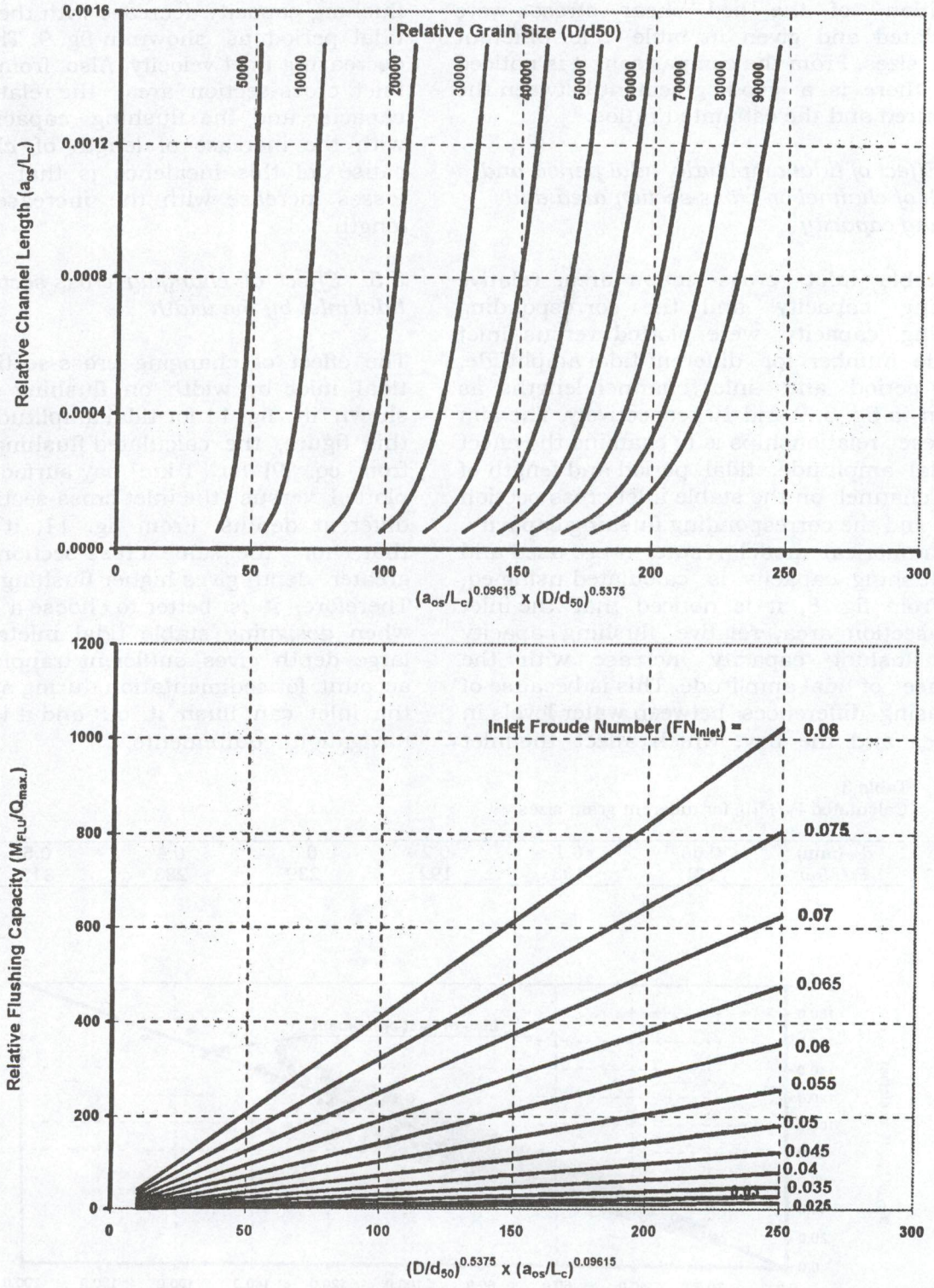

Fig. 7. Applicable curves for calculation of relative flushing capacity of tidal inlets, ($M_{Flu}/Q_{max.}$), using eq. (9).

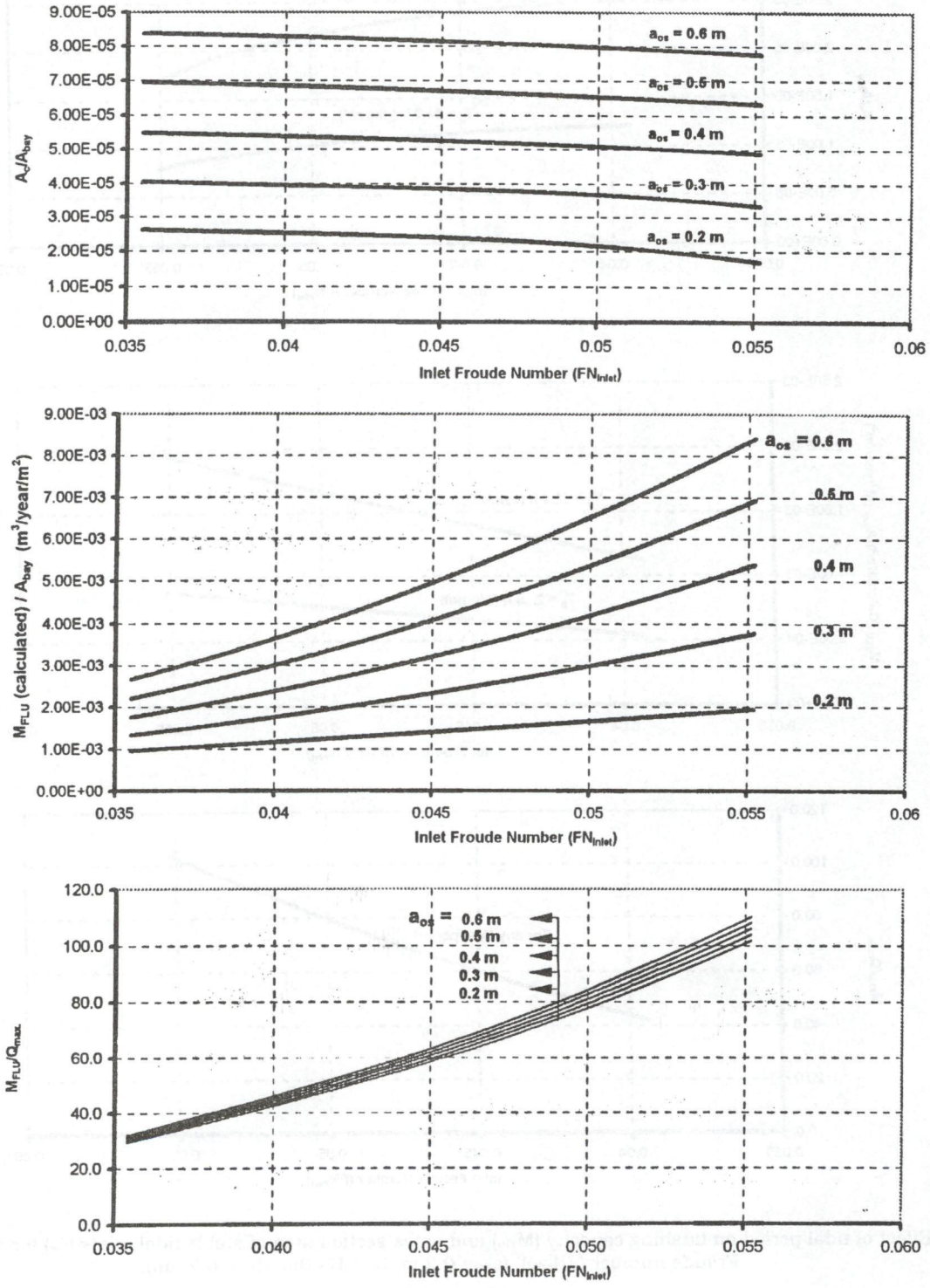

Fig. 8. Effect of tidal amplitude on flushing capacity (M_{Fiu}) and cross-section area of stable tidal (A_c) for different inlet Froude number (FN_{Inlet}), (L_c= 1000m, T_p =12.4 h, d_{50} = 0.2 mm).

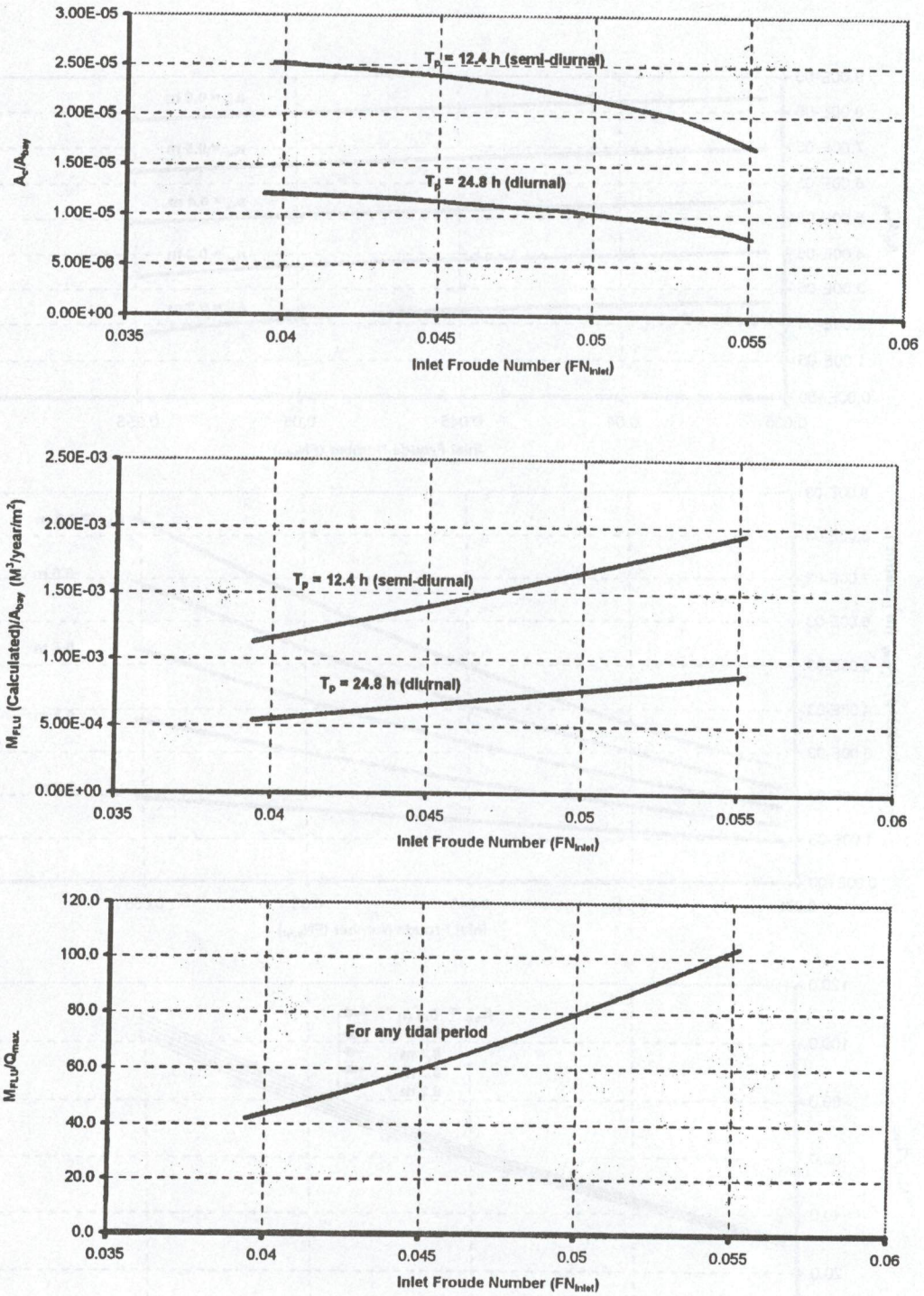

Fig. 9. Effect of tidal period on flushing capacity (M_{Flu}) and cross-section area of stable tidal inlets (A_c) for different inlet Froude number (FN_{inlet}), (a_{os} = 0.2 m, L_c = 1000m, d_{50} = 0.2mm).

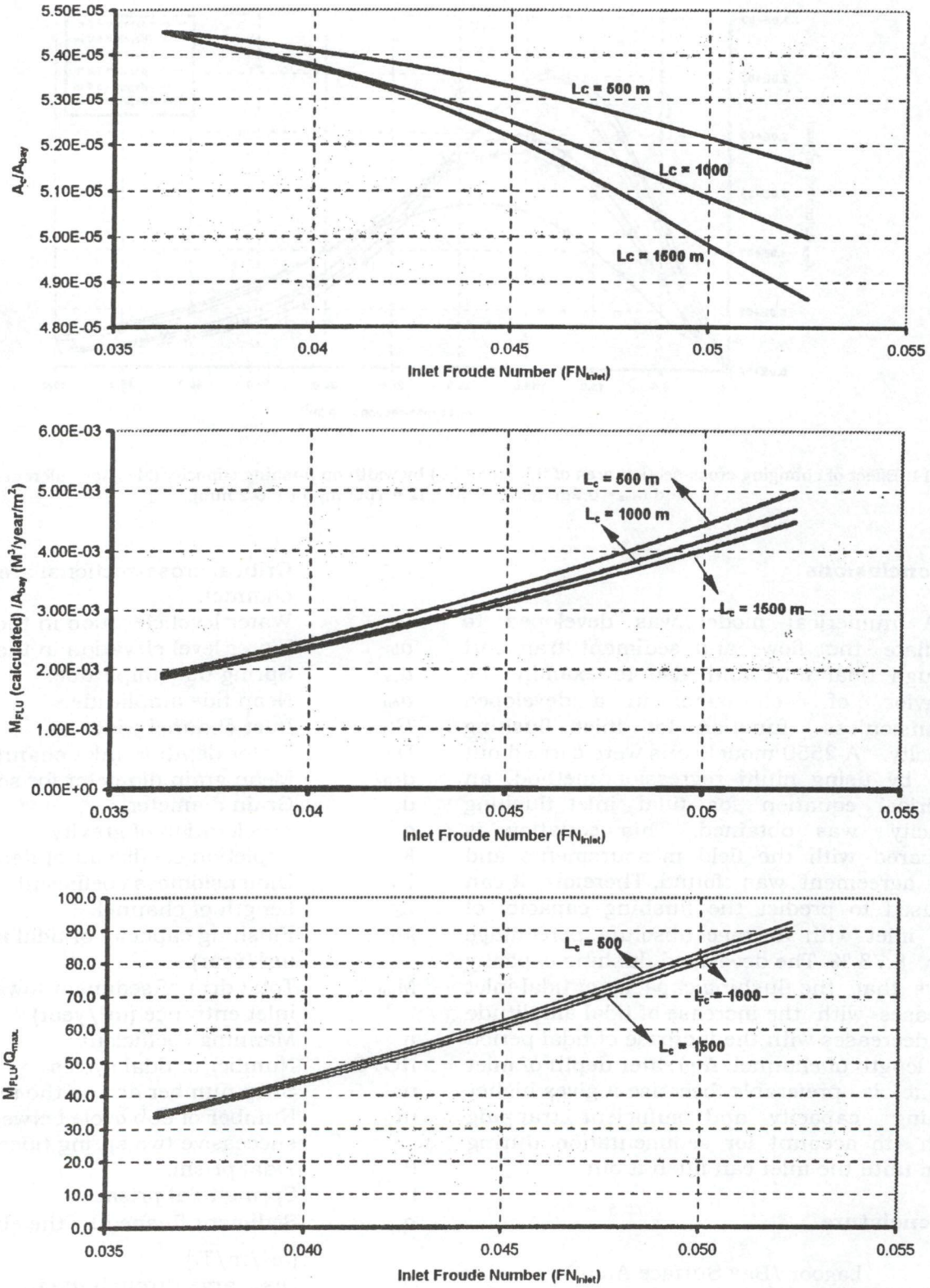

Fig. 10. Effect of length of inlet channel on flushing capacity (M_{Flu}) and cross-section area of stable inlets (A_c) for different inlet Froude number (FN_{inlet}),(a_{os}=0.4m, T_p=12.4 h, d50 = 0.2mm).

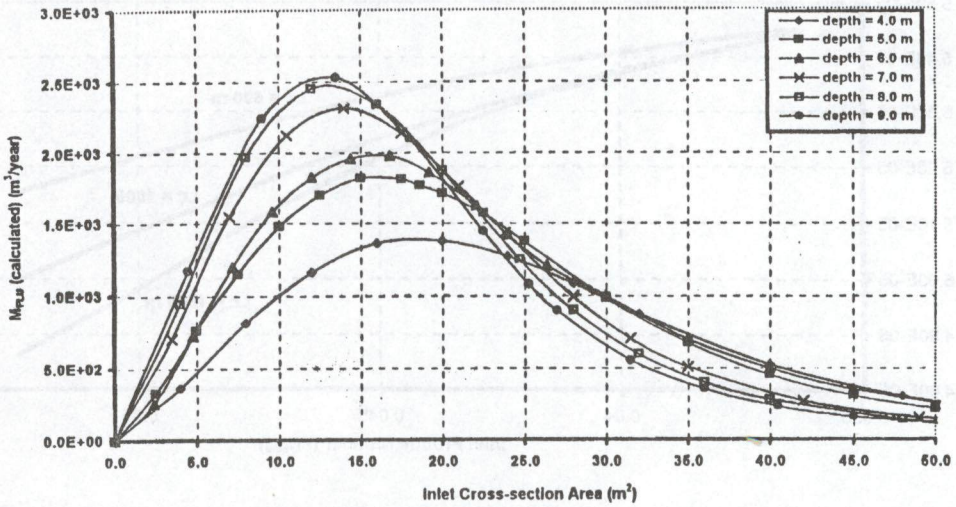

Fig. 11. Effect of changing cross-section area of tidal inlet (A_c) by width on flushing capacity (M_{Flu}) for different depths (D), and (a_{os} = 0.2m, A_{bay} = 1 km², L_c = 1000m, d_{50} = 0.2 mm).

6. Conclusions

A numerical model was developed to simulate the flow and sediment transport through tidal inlet and also to examine the behavior of each factor in a developed dimensionless function for inlet flushing capacity. A 2550 model runs were carried out and by using multi regression method, an empirical equation for tidal inlet flushing capacity was obtained. This equation is compared with the field measurements and good agreement was found. Therefore, it can be used to predict the flushing capacity of tidal inlet with average absolute percentage error 8.73 %. The developed flushing capacity shows that the flushing capacity of tidal inlet increases with the increase of tidal amplitude and decreases with the increase of tidal period and length of channel. A greater depth of inlet channel is preferable, because it gives higher flushing capacity and sufficient trapping depth to account for sedimentation during storm until the inlet can flush it out.

Nomenclature

A_{bay}	Lagoon/Bay Surface Area.
A_c	Cross-sectional area of inlet channel.
A_c^*	Critical cross-sectional area of inlet channel.
a_s	Water level elevation in the sea.
a_b	Water level elevation in the bay.
a_{os}	Spring tide amplitude.
a_{on}	Neap tide amplitude.
B	Inlet channel width.
D	Water depth in inlet channel (m).
d_{50}	Mean grain diameter for sediment.
d_s	Grain diameter.
g	Acceleration of gravity.
K	Repletion coefficient of Keulegan.
K_s	Dimensionless coefficient
L_c	Length of channel.
M_{FLU}	Flushing capacity of tidal inlet (m^3/year).
M_{tot}	Total drift of sediment towards the inlet entrance (m^3/year).
n	Manning coefficient.
NOTC	Number of tidal cycles
ns	Strip number across the inlet width.
nt	Number of ebb cycle between successive two spring tides.
P	Tidal prism.
P_s	Spring tidal prism.
q_{s_i}	Sediment flushed by the ebb flow ($m^3/m/T_e$).
Q_i	Discharge through inlet.
Q_t	Total discharge through multiple inlets.

Q_f	Discharge into the bay from other sources such as (rivers, pumped inflows, etc.).
R_c	Hydraulic radius.
s	Relative density of sediment.
T_p	Tidal period.
T_e	Ebb time as a part of the tidal period.
T_l	Lunar period.
u	Average flow velocity in the inlet.
$V_{max.-mean}$	Maximum mean inlet velocity.
ρ	Density of water.
ρ_s	Density of sediment.
υ	Kinematic viscosity coefficient.
ω	Frequency of tidal motion.

References

[1] F. F. Escoffier," The stability of tidal inlets", Shore and Beach, Vol. 8 (4), p.114 (1940).

[2] P.Bruun," Stability of Coastal Inlets", Elsevier Scientific Pub. Co., Amsterdam, p.510 (1978).

[3] V.d. Kreeke's," Stability of tidal inlets" Estuarine, Coastal and Shelf Science, Pass Cavallo, Texas. Vol. 21 (1), pp. 33-43 (1985).

[4] F. Engelund and E. Hansen," A monograph of sediment transport in alluvial channels", Danish Press, Copenhagen (1967).

[5] L.C. Van-Rijn," Sediment transport, part i: bed load transport", J. of Hydr. Eng., Vol. 110 (10) (1984).

[6] L.C. Van-Rijn," Sediment transport, part ii: suspended load transport", J. of Hydr. Eng., Vol. 110 (11) (1984).

[7] L.C. Van-Rijn," Sediment transport, part iii: bed forms and alluvial roughness," J. of Hydr. Eng., Vol. 110 (12) (1984).

[8] P. Bruun, F. Gerritsen & N.P. Bhakta," Evaluation of overall entrance stability of tidal entrances", Proceeding of 14.th Coastal Engineering Conference, ASCE, pp.1566-1584 (1974).

[9] Coastal Research Institute," Monitoring The Effects of El-Bardawil Lagoon Protection Works on its Boughazes and Adjacent Areas," Progress Technical Report No.1 for the period from (June to October 1999) (1999).

[10] M.P. O'Brien & R.R. Clark R.R.," Hydraulic constant of tidal entrances,"14.th Coastal Engineering Conference, Copenhagen, Vol. II, pp. 1546-1565 (1974).

[11] A. Skou," On The Geometry of Cross-Section Areas in Tidal Inlets." Ph. D. Thesis Submitted to The Institute of Hydrodynamics and Hydraulic Engineering, Technical University of Denmark (1990).

Received September 1, 2001
Accepted October 20, 2001